MR-guided adaptive focusing of therapeutic ultrasound beams in the human head.

Laurent Marsac, Dorian Chauvet, Benoît Larrat, Mathieu Pernot, Benjamin Robert, Mathias Fink, Anne-Laure Boch, Jean-François Aubry, Mickaël Tanter

MR-guided adaptive focusing of therapeutic ultrasound beams in the human head

Laurent Marsac [1 2 *] , Dorian Chauvet [3] , Benoît Larrat [3] , Mathieu Pernot [3] , B. Robert [3] , Mathias Fink [3] , Anne-Laure Boch [3] ,
Jean-François Aubry [3] , Mickaël Tanter [3]

[1] *Physique des ondes pour la médecine INSERM : U979 , Université Paris VII - Paris Diderot , CNRS : UMR7587 , ESPCI ParisTech ,
Institut Langevin ondes & images, 10 rue Vauquelin 75231 PARIS Cedex 05,FR*

[2] *Supersonic Imagine , Les jardins de la Durance, 510 rue René Descartes 13857 Aix en Provence,FR*

[3] *Service de neuro-chirurgie Assistance publique - Hôpitaux de Paris (AP-HP) , Hôpital Pitié-Salpêtrière , Université Paris VI - Pierre et
Marie Curie , 47-83, boulevard de l'Hôpital 75651 PARIS Cedex 13,FR*

* Correspondence should be adressed to: Laurent Marsac <laurent.marsac@gmail.com >

Abstract
Purpose

This study aims to demonstrate, using human cadavers the feasibility of energy-based adaptive focusing of ultrasonic waves using
Magnetic Resonance Acoustic Radiation Force Imaging (MR-ARFI) in the framework of non-invasive transcranial High Intensity
Focused Ultrasound (HIFU) therapy.

Methods

Energy-based adaptive focusing techniques were recently proposed in order to achieve aberration correction. We evaluate this
method on a clinical brain HIFU system composed of 512 ultrasonic elements positioned inside a full body 1.5 T clinical Magnetic
Resonance (MR) imaging system. Cadaver heads were mounted onto a clinical Leksell stereotactic frame. The ultrasonic wave
intensity at the chosen location was indirectly estimated by the MR system measuring the local tissue displacement induced by the
acoustic radiation force of the ultrasound (US) beams. For aberration correction, a set of spatially encoded ultrasonic waves was
transmitted from the ultrasonic array and the resulting local displacements were estimated with the MR-ARFI sequence for each
emitted beam. A non-iterative inversion process was then performed in order to estimate the spatial phase aberrations induced by the
cadaver skull. The procedure was first evaluated and optimized in a calf brain using a numerical aberrator mimicking human skull
aberrations. The full method was then demonstrated using a fresh human cadaver head.

Results

The corrected beam resulting from the direct inversion process was found to focus at the targeted location with an acoustic intensity
2.2 times higher than the conventional non corrected beam. In addition, this corrected beam was found to give an acoustic intensity
1.5 times higher than the focusing pattern obtained with an aberration correction using transcranial acoustic simulation based on
X-ray computed tomography (CT) scans.

Conclusion

The proposed technique achieved near optimal focusing in an intact human head for the first time. These findings confirm the strong
potential of energy-based adaptive focusing of transcranial ultrasonic beams for clinical applications.

Author Keywords MRI ; adaptive focusing ; MR-ARFI ; ultrasound transcranial therapy ; HIFU

INTRODUCTION

Transcranial adaptive focusing of therapeutic ultrasonic waves remains a challenging problem in the field of medical ultrasound: the
heterogeneities of biological tissue and skull bone in terms of speed of sound, density and ultrasonic attenuation induce a distortion of the
ultrasonic wave field[1]. This distortion results in partial destruction of the focusing pattern. In order to restore focusing quality, adaptive
focusing relies on the use of ultrasonic arrays to correct the distortions induced by the propagation medium. This correction is performed
by estimating and applying different time shifts (or phase shifts for monochromatic waves) on each element of the array. In some
situations, when the ultrasonic array incorporates both transmit and receive channels, it may be possible to rely on the echoes of a bright
reflector or a point-like active source located inside the biological tissues[2]. From the signals received on the array (corresponding to the
Green's function) one can time reverse the wave field[3 ,4] (or phase conjugate for monochromatic signals[5]) to focus back on the initial
position. However, the direct measurement of the Green's function between the target location and the ultrasonic array is not possible in
the brain under practical clinical conditions. One way to estimate the Green's function in this situation is to simulate acoustic propagation
through the skull by finite difference time domain method using prior determination of its density and speed of sound at each point based

on CT scans[6 ,7]. However such simulations rely on a model, measured parameters and numerical approximations that can induce errors in the estimation.

To overcome this problem, we have recently introduced a novel method called energy-based adaptive focusing[8 –10]. The general principle, which can be applied to any kind of waves in physics, relies on the indirect estimation of wave intensity at the target for different coded excitations in order to determine the phase shifts which provide the best correction for aberrations. By transmitting Hadamard-coded signals with an array of transducers and estimating the beam intensity at the target, this approach was shown to achieve direct and accurate phase aberration correction without any phase measurement. In medical ultrasound, ultrasonic waves interact with biological tissues through physical effects linked to wave intensity such as acoustic radiation force or tissue heating due to the absorption of ultrasound. Thus, the quantitative measurement of tissue displacement or temperature elevation at the target can be used for the indirect estimation of local beam intensity.

Due to momentum transfer from the acoustic wave to the medium, the radiation force induced by a short sonication (~ 100 μ s) generates a local tissue displacement of several tens of micrometers at the focus of the US beam. The use of displacements induced by the acoustic radiation force of the ultrasonic beams for adaptive focusing was previously demonstrated[11]. Herbert *et al.* improved the method by using auto-correction: the ultrasonic array was able to both transmit a coded excitation and to estimate the resulting displacements at the targeted location using ultrasonic backscattered echoes[9]. However, although this concept is interesting, it cannot be directly applied transcranially because the strong attenuation of the skull bone considerably lowers the US imaging performance. In such cases, another imaging modality is required to provide an indirect estimation of the beam energy at the target.

For transcranial applications, Magnetic Resonance (MR) imaging is most appropriate for guiding the energy-based adaptive focusing technique. Motion sensitive MR sequences have been previously developed to map micrometric displacements induced by the acoustic radiation force in biological tissue and called MR-ARFI sequences[12 –15]. In these sequences the displacement is encoded in the phase of the reconstructed MR images. Such MR displacement measurement was later used for adaptive focusing using Hadamard-coded signals[10]. Recently, Hertzberg *et al.* evaluated an iterative approach and a direct inversion procedure, in 5 % fatted milk yoghurt and through a human skull bone in water, with 172 elements of a transducer operating at 710 kHz. They achieved a displacement increase compared to a CT simulation based correction and reached 90 % of the optimal displacement[16]. MR-ARFI adaptive focusing is particularly interesting for HIFU applications for two reasons. On the one hand, most available technologies are based on therapeutic arrays used only in transmit mode, so that the estimation of tissue displacement has to be performed by another imaging modality. On the other hand, many HIFU therapeutic applications are already being performed under MR guidance, such as uterine fibroids[17], prostate[18], breast[19 ,20] or brain [21]. For brain applications, MR guidance is even mandatory as no other imaging modality can provide a high level 3D delineation of tumor margins for treatment planning and monitoring of temperature elevation during treatment.

In this paper, our aim is to achieve energy-based adaptive focusing in a configuration that closely mimics expected future clinical conditions. Thus, we demonstrate on a human cadaver head and using a clinical brain HIFU system (SuperSonic Imagine, Aix en Provence, France) that MR-ARFI adaptive focusing of transcranial HIFU beams can be used prior to treatment to reach optimal focusing.

MATERIALS & METHODS

High power therapeutic system

A 1 MHz, 512 element HIFU array (Imasonic, France) dedicated to human transcranial brain hyperthermia (Fig. 5) was employed. The elements were oriented as plotted on [Fig. 3(a,b)]. This probe is partially spherical (15 cm focus and 23 cm aperture) in order to focus the acoustic energy at the geometrical focus. The elements are circular with a 6 mm diameter to fit the skull correlation length at 1 MHz and their maximum acoustic intensity is 20 W/cm^2 . They are oriented in non periodic geometry in order to lower grating lobes while permitting a tight ellipsoidal focalization pattern (half-pressure beam dimension of 1.5 mm laterally and 5 mm axially). The 384 elements of the probe used in this study are plotted as circles in [Fig. 3(a)] and the 128 square marks correspond to the unused elements. The array is composed of non-ferromagnetic materials to avoid imaging artifacts during MR-guided experiments.

Coupling to the sample of interest was achieved through degassed water maintained by a 0.2 mm thick latex membrane. Echographic gel was also used at the membrane-sample interface to improve acoustic coupling. The head or sample of interest was immobilized in a stereotactic frame with screws. This frame is mounted on a non-ferromagnetic head holder incorporating three degrees of freedom (the probe holder provides three additional degrees of freedom for the probe). Both holders have discrete positioning systems that enable a choice of predefined fixed positions.

Initial pressure measurements of the probe were made in a degassed water tank using a calibrated hydrophone (HNA400, Onda, USA) in order to evaluate intensity at focus for reference. The hydrophone was placed at the probe focus using a 3D positioning system (precision ± 0.1 mm) and the 384 emitting elements used in the study were driven with the same phase during 10 μ s. The hydrophone signal was recorded with a digital oscilloscope (Tektronix, Beaverton, OR, USA) and the peak pressure generated by the system was

measured at the fundamental frequency. Pressures for adaptive focusing experiments were estimated by taking into account losses due to the coupling membrane, skull and brain within the linear hypothesis. The coupling membrane attenuation was previously measured to be 1.4 dB at 1 MHz by a transmission measurement method using two transducers. The values of attenuation measured were 11 dB for the skull and 2.5 dB for the brain (50 mm of brain with a brain attenuation of 0.05 dB/mm). The total probe output power was 1350 acoustic watts in free field conditions.

MR acquisitions

All MR acquisitions were made with a 1.5 T Philips Achieva scanner. RF acquisition was achieved by standard commercial Flex® surface coils. A dedicated MR-ARFI sequence was developed by adding two motion sensitizing gradient (MSG) modules before and after the π pulse of a standard multislice spin-echo sequence with echo planar imaging (EPI) readout. Each MSG module was a bipolar rectangular of opposite polarity, as indicated on the sequence chronogram in Fig. 1 . Three contiguous slices oriented perpendicularly to the US beam were simultaneously acquired and the resolution was set to $2 \times 2 \times 7$ mm³ (Matrix 96×26, FOV 160 mm × 72 mm). Two lateral saturation slices were used in the phase encoding direction to prevent signal overlapping. The sequence parameters were: TE = 70 ms, TR = 1.2 s, EPI factor 13, resulting in a 2.4 s acquisition time. The MSGs were placed along the slice selection axis to ensure proper displacement encoding. Each rectangular lobe lasted 5 ms with a plateau maximum strength of 41 mT/m. For each TR, two triggering pulses were sent by the MR scanner to the US electronic boards in order to synchronize the US emissions relative to the MR displacement encoding. They were placed at the beginning of the second halves of each MSG module as indicated in Fig. 1 . This choice was made in order to avoid encoding residual displacement during the other halves of the MSG periods. For each trigger, the duration of sonication was adjusted to 5 ms which represented a good compromise between motion sensitivity and limited US duty cycle.

Sonications were made twice per MR EPI shot: once during the negative part of G1 and once during the positive part of G2. In the 26 line image, the EPI acceleration factor was 13 so one image required 2 MR EPI shots. This led to 4 sonications per image. Therefore, 12 sonications were needed to acquire the 3 slices imaged by the MR-ARFI sequence. For each differently encoded US emission of the adaptive focusing experiment, two MR-ARFI images were acquired: one without and one with sonication as shown for the calf brain case on [Fig. 2(a)–(b)]. Encoded displacement maps were computed by subtracting the phase images obtained respectively with and without sonication, as shown in [Fig. 2(c)]. This compensates for any drift of the MR scanner during the adaptive focusing experiment.

For each adaptive focusing process, the signal to noise ratio (SNR) was computed using the voxel at the target location of all MR-ARFI acquisitions. The signal was computed as the mean of the 1536 encoded displacements. The noise computation was the standard deviation of the 1536 reference phases (without sonications).

Energy-based adaptive focusing

Optimal focusing through an arbitrary phase aberrating medium can be achieved by measuring the acoustic intensity at a chosen target location inside the medium for a finite set of coded US emissions with a direct inversion[9 ,10]. While this is in theory feasible, an absolute measurement of the acoustic intensity is not direct and requires assumptions. Here we directly rely on MR-ARFI encoded tissue displacement which is assumed to be linearly dependent on the acoustic intensity at the probe focus[10]; this was verified in the calf brain experiment.

As previously described[9], the technique consists of using a Hadamard basis to determine 384 virtual elements. By considering two virtual emitters *A* and *B* with *B* having a phase aberrator in front of it, one can measure the intensity of the interference pattern at a desired target and tune the emitted phase of *B* to reach optimal focusing. It has been shown that four different phase emissions are sufficient to reveal their phase shift[9]. This step was undertaken for a fixed virtual emitter *A* and all virtual emitters *B* which led to 384 phase shifts corresponding to the aberrator of the virtual emmiters. To compute the phase aberration of the actual aberrator we then performed a basis transformation using the inverse of the Hadamard matrix in order to return to the canonical basis.

The adaptive focusing process used the 1536 Hadamard coded US emissions described above (384×4). In order to realize the MR-ARFI measurements a total of 18432 US sonications were made (1536×12). Each US sonication consisted of a 5 ms continuous wave signal. All sonications had the same acoustic power. Total acquisition time for the whole adaptive focusing procedure was 2 hours and thus the average duty cycle for the ultrasound emissions was approximately 1.25 %.

Calf brain experiment using virtual aberration

In the first experiment the proposed adaptive focusing technique was tested *ex vivo* on freshly excised calf brains. They were embedded in 3 % agar phantom gels to ease the positioning of the sample at the geometrical focus of the US probe. The phantoms were prepared with degassed water and special care was given to avoid trapping air bubbles at the gel-brain interface. In order to determine the probe focus location in the calf brain, sagittal and transverse standard anatomical images were acquired using a T1 MRI pulse sequence (TE 2.3 ms, TR 5.1 ms, voxel size $1.7 \times 1.7 \times 2$ mm³). On the sagittal image, the probe, MR-ARFI imaging plane and probe focus are represented in [Fig. 3(b)]. On top of the transverse image, the MR-ARFI field of view and probe focus are shown on [Fig. 3(c)].

The duration of the encoded pulse was set to 5 ms in order to have enough signal and to avoid significant heating. We first performed an initial verification of the linear dependence of the encoded displacement with respect to the acoustic power. Using a US emission with all elements in phase, we measured the encoded displacement at the probe focus for several acoustic spatial peak intensities between 142 W/cm^2 and 3565 W/cm^2 .

Once the linear relationship was established, we performed the adaptive focusing. In this setup, no physical phase aberrator was introduced between the array and the brain. In order to evaluate the adaptive focusing technique, virtual realistic skull aberration phases plotted on [Fig. 3(a)] were electronically added to all the US emissions of the experiment. These phases were obtained from a previous hydrophone measurement at the brain therapy probe focus through a degassed *ex vivo* human skull. This measurement was made in a water tank using geometrical positioning of the probe and skull similar to that of brain therapy treatment. The skull used for phase measurement had a thickness of 8.3 mm on average, and was obtained from a 80 year old donor. Angles between skull external surface normals and individual transducers axes were 8 degrees on average. The adaptive focusing process was then performed as described above and finally the encoded displacements were measured for the US emission with virtual aberration, with no aberration and with virtual aberration plus energy-based adaptive focusing correction.

Human brain experiment in head using the skull aberration

A second set of experiments were undertaken using one fresh human cadaver head as approved by the ethics committee of the Centre du Don des Corps (René Descartes University, Paris). The head was removed at the Institut d'Anatomie (UFR Biomédicale des Saints-Pè res, René Descartes University, Paris) 48 hours after death. A clinical Leksell stereotactic frame (Elekta, Stockholm, Sweden) was fixed on the head with screws as illustrated in (Fig. 5). We used the same elements of the probe as for the calf brain experiment but in this case no virtual aberration was added: the aberrations were induced by the skull itself. In this experiment, a lower pressure was reached at the focus due to skull attenuation which is between −9 dB to −15 dB at 1 MHz[1], so we assumed that the encoded displacement was still linear with the acoustic power. We targeted the interthalamic adhesion tissues in the third ventricle. Fig. 4 shows the MR-ARFI slice positioning and target location on top of a conventional anatomic T1 MR image.

In the first experiment, the adaptive focusing process was performed as described above and the encoded displacements were measured for the US emission without correction, with simulation-based aberration correction and with energy-based adaptive focusing correction.

In a second experiment the simulation-based correction was used as a pre-correction for a new energy-based adaptive focusing process, the aim was to increase the SNR in order to obtain a more accurate correction.

Finite differences simulations

Simulation of wave propagation through the skull up to the probe was performed in order to non-invasively obtain an aberration correction reference. The 3D simulation used second order finite differences time domain (FDTD) computations and was performed using an acoustic model of the skull developed in previous studies[22]. The skull acoustic properties were obtained from a CT scan of the head having a 0.3 mm in slice resolution and 0.5 mm inter-slice resolution. The simulation spatial step was set to a tenth of a wavelength at 1 MHz (0.15 mm) and the time step was set to 20 ns in order to satisfy Von Neuman stability conditions. The full volume was 1500 × 1500 × 600 voxels and the simulation time was 3 hours using a dual Xeon, 24 GB memory computer. Further information about the procedure can be found in previous studies[23 ,24].

Impact of the MR-ARFI SNR on adaptive focusing

One way to evaluate the impact of the SNR is to numerically add noise on the MR measurements, estimate the corresponding US correction phases and analyze the theoretical intensity variation at focus. In the human head the adaptive focusing process using the simulation based solution as a pre-correction led to optimal focusing. Numerical pseudo-random Gaussian noise with different standard deviations (in order to have a SNR between 4 and 8.3) were added to the MR encoded displacement of the adaptive focusing process. The corresponding phase corrections were computed for each numerical noise value. The intensity loss relative to the optimal focusing was then computed for the different phase corrections allowing an estimate of the intensity loss for each numerical noise value.

RESULTS

Acoustic power

The hydrophone pressure measurement at the focal probe led to estimations respectively of 6.2 MPa for the calf brain and 2.3 MPa for the cadaver head experiments. The spatial peak acoustic intensities at focus were deduced to be respectively 1300 W/cm^2 and 172 W/cm^2 . The estimated acoustic power at the focus within the calf brain and the human head was estimated to be lower than 0.3 W on average for the whole experiment, thus the brain temperature was assumed to remain constant.

Adaptive focusing in calf brain

Encoded displacement in the calf brain was verified to increase linearly with the acoustic power. The maximum encoded displacement was obtained for the first Hadamard vector because in this particular case all elements are emitting in phase [Fig. 6(a)]. Examples of encoded displacement for other Hadamard vectors [Figs. 6(b)–(d)] illustrate the displacement variation at the focus from one vector to another. The SNR was estimated to be 20.2.

Each of the 1536 Hadamard coded sonications led to measurable displacement. Once they were complete and the aberration correction computed at the targeted voxel, the encoded displacement was measured and plotted for all three cases. In Fig. 7(a) with aberration, Fig. 7(b) without aberration, Fig. 7(c) with aberration and correction. The maximum displacement was found to be at the desired location in all three cases. As shown on the lateral profile of the slices in Fig. 7(d) , the adaptive focusing technique increased the displacement by 48.4 % relative to the emission with virtual aberration, and by 14.6 % relative to the emission without aberration. This first experiment demonstrates that the aberrations were fully recovered and that energy-based adaptive focusing is an improvement over focusing obtained without aberration and with in-phase emissions.

Adaptive focusing in human head

In the human head experiment, the encoded displacement was measured for the following three cases: no correction [Fig. 8(a)], with simulation-based correction [Fig. 8(b)] and with energy-based adaptive focusing correction [Fig. 8(c)]. In all three cases, maximum displacement was found to be at a distance to the targeted voxel not greater than half the wavelength (0.75 mm). As shown in Fig. 8 the energy-based adaptive focusing technique increased displacement by 86.8 % relative to the uncorrected emission but the displacement was 22.3 % lower than the emission based on simulation correction.

The reflection occurring at the skull surface combined with the bone and brain tissue attenuation strongly decreases acoustic intensity at the focus. The average encoded displacement at the focus of all emissions was 71 % lower than in the calf brain, this led to an estimated SNR of 5.9. This decrease in SNR was assumed to lower the quality of the correction estimation. It might explain why the adaptive focusing correction applied without any a priori knowledge had a lower performance than the simulation based correction. One way to test this assumption was to increase the average encoded displacement of all emissions using a pre correction.

The simulation-based correction was used as a pre-correction for a new energy-based adaptive focusing experiment using a priori information. The average encoded displacement of all emissions at the target was 59 % lower than in the calf brain, this led to an estimated SNR of 8.3. As in the previous experiment, the encoded displacement was measured for the three following cases: no correction [Fig. 9(a)] , with simulation based correction [Fig. 9(b)] and with energy-based adaptive focusing correction using the a priori simulation pre-correction [Fig. 9(c)].

As visible on the lateral profile of the slices shown in Fig. 9(d) , the adaptive focusing technique increased displacement by 218 % relative to the uncorrected emission and by 48.6 % relative to the simulation based correction alone. This demonstrates that the energy-based adaptive focusing technique can reach better aberration correction than the simulation based correction. One conclusion is that a 5.9 SNR is not enough to ensure the efficiency of the adaptive focusing process. It also shows that a minimum SNR is mandatory if the technique is to be performed successfully. In this case the minimum required SNR seems to be higher than 5.9 and lower than 8.3. In addition simulation based transcranial correction were previously shown to reach 69 % intensity (83 % in pressure) of the optimal focusing [24]. Here the gold standard cannot be measured but the intensity obtained with the simulation based correction is 67 % of the energy-based adaptive focusing. This suggests that the proposed method may achieve a near-optimal focusing.

Impact of the MR-ARFI SNR on adaptive focusing

Estimated acoustic intensity relative to optimal focusing intensity is shown in Fig. 10 . Using the energy-based adaptive focusing technique (without prior correction), the SNR was 5.9 and the intensity after correction was 53 % of the optimal correction. Thus this adaptive focusing based on a 5.9 SNR correlates well with the estimation of Fig. 10 . Using this estimation we can deduce that a SNR higher than 8 should be reached in order to obtain a near optimal focusing.

DISCUSSION

The concept of spatially encoded excitations such as Hadamard vectors developed in this study is the key for working with a large number of transducers. Compared to recent work performed on 172 independent elements[16], we were able to correct phase aberrations on 384 independent elements with reasonable acquisition time by using this approach.

Optimal focusing was first demonstrated in the calf brain using numerical phase aberrations previously measured from a real *ex vivo* human skull. Energy-based adaptive focusing was able to fully compensate for the phase aberrations. Compared to the experiment performed without any phase aberration, energy based adaptive focusing was even able to increase the acoustic intensity at the focus by

14.6 %. This result confirms previous observations made by Larrat *et al.* using a small animal high field 7 T MR system[10]. Thus the technique allows optimal correction not only of the numerical phase aberrations, but also of all other uncontrolled sources of phase aberrations including probe-to-sample transmission medium, tissue heterogeneities, errors on the geometrical focus localization, small defects in the transducer geometry or mechanical accuracy and electronic phases.

A 20.2 MR-ARFI SNR was obtained in the calf experiment, which allowed us to investigate the accuracy of the adaptive focusing technique. However, in the cadaver head experiment, strong reflection and attenuation of the ultrasonic wave induced by the skull considerably decreased acoustic intensity in the brain. The MR-ARFI SNR was therefore much lower in the cadaver head experiment. With an SNR of 5.9, the sole energy-based adaptive focusing technique (without prior correction based on CT scan) allowed us to improve the acoustic intensity by 86 % at the focus. Finally, by using non-optimal simulation-based correction as the initial emission signals, an SNR of 8.3 was obtained and the near optimal acoustic intensity reached a 218 % increase. In order to achieve the energy-based adaptive focusing we found the required SNR must be in the range between 5.9 and 8.3. The minimal SNR was estimated to be 8. There are several options to increase the SNR. One possibility consists in increasing the acoustic power. For example, if all the 512 elements of the probe could be used instead of 384, the SNR would rise to 10.5, leading to optimal focusing without simulation-based corrections. Novel MR sequences with higher sensitivity could also be investigated in the future in order to increase the SNR. Nevertheless the acquisition time of such sequences should not exceed a few seconds for future clinical use (as a reference, 2.4 s acquisition time was achieved in this study).

Reducing acquisition time is of interest because it could make this technique suitable for clinical investigations. In this study, the total acquisition time was 2 hours which is still long for clinical studies. However, the acquisition time could be reduced by further optimization of the MR sequence and by decreasing the number of vectors used in the adaptive focusing process. This can be done by acquiring only the Hadamard vectors containing the spatial frequency content of the aberrating skull[10] or by using other adapted vectors (such as the Walsh basis which sorts Hadamard vectors with increasing spatial frequency). Further work will focus on these optimizations in the hope of dramatically reducing acquisition time.

This study illustrates the strong potential of this technique in transcranial MR-guided HIFU applications for both aberration correction and precise localization of the focus in the brain. This technique has several potential advantages over previous techniques based on CT images[5 ,25]. First, it greatly eases protocol. Indeed, the whole treatment procedure can be performed using MR guidance, thus avoiding the requirement for CT scan acquisition prior to treatment coupled to finite differences. Secondly, it eases treatment planning and especially the targeting accuracy: compared to the 3 different referential frames used today (MR planning, CT planning and MR monitoring during the treatment) which can introduce many small positioning errors, a single referential frame would be necessary (the MR referential providing both planning and monitoring). Thirdly, this technique could accelerate the aberration correction process: it could be performed in a short acquisition time (typically 20 to 30 minutes immediately prior to treatment) with the patient in their clinical treatment setup. For this reason, this approach could be particularly suitable for stroke treatments where the time to treatment is a major issue. Fourthly, the method provides a direct image of the focus location as well as the efficiency of the correction. This should result in better safety control and focusing quality estimation prior to the treatment. Lastly, this method uses only experimental measurements to provide the optimal focusing beam, thus reducing theoretical assumptions about wave propagation. Contrary to all other approaches based on simulations that rely on many assumptions about the medium properties, it provides a real correction for skull, brain and coupling medium in any kind of complex configurations.

In this study, energy-based adaptive focusing of ultrasonic waves is achieved for the first time in a human head under MR guidance. Using a clinical setup, we demonstrated that energy-based adaptive focusing can successfully achieve optimal focusing and restore sharp focus in the human brain. By implementing further acceleration and measurement optimization, this could create more accurate HIFU treatments of central regions of the brain such as thalamus or hypothalamus for neuropathic pain, essential tremors or others pathologies.

Acknowledgements:

References:

- 1 . Fry FJ , Barger JE . Acoustical properties of the human skull . J Acoust Soc Am . 63 : 1576 - 1978 ;
- 2 . Flax SW , O'Donnell M . Phase-aberration correction using signals from point re ectors and diffuse scatterers: basic principles . IEEE Trans Ultrason Ferroelectr Freq Control . 35 : 758 - 1988 ;
- 3 . Thomas J-L , Fink MA . Ultrasonic beam focusing through tissue inhomogeneities with a time reversal mirror: application to transskull therapy . IEEE Trans Ultrason Ferroelectr Freq Control . 43 : 1122 - 1996 ;
- 4 . Tanter M , Thomas JL , Fink M . Focusing and steering through absorbing and aberrating layers: application to ultrasonic propagation through the skull . J Acoust Soc Am . 103 : 2403 - 1998 ;
- 5 . Clement GT , White J , Hynynen K . Investigation of a large-area phased array for focused ultrasound surgery through the skull . Phys Med Biol . 45 : 1071 - 2000 ;
- 6 . Clement GT , Hynynen K . Micro-receiver guided transcranial beam steering . IEEE Trans Ultrason Ferroelectr Freq Control . 49 : 447 - 2002 ;
- 7 . Aubry JF , Tanter M , Pernot M , Thomas JL , Fink M . Experimental demonstration of noninvasive transskull adaptive focusing based on prior computed tomography scans . J Acoust Soc Am . 113 : 84 - 2003 ;

- 8 . Pernot M , Tanter M , Fink M , Tanter M , Montaldo M , Aubry JF , Sinkus R . Waves focusing optimizing method for use in e.g. therapy, involves deducing optimal distribution of emission phase and amplitude distribution from disturbance measurement to maximize disturbance induced in focus zone . International Patent . PCT/FR20070001235 February 21 2007 ;
- 9 . Herbert E , Pernot M , Montaldo G , Fink M , Tanter M . Energy-based adaptive focusing of waves: application to noninvasive aberration correction of ultrasonic wavefields . IEEE Trans Ultrason Ferroelectr Freq Control . 56 : 2388 - 2009 ;
- 10 . Larrat B , Pernot M , Montaldo G , Fink M , Tanter M . Mr-guided adaptive focusing of ultrasound . IEEE Trans Ultrason Ferroelectr Freq Control . 57 : 1734 - 2010 ;
- 11 . Urban MW , Bernal M , Greenleaf JF . Phase aberration correction using ultrasound radiation force and vibrometry optimization . IEEE Trans Ultrason Ferroelectr Freq Control . 54 : 1142 - 2007 ;
- 12 . Sinkus R , Siegmann K , Pernot M , Athanasiou A , Fink M . Potential of mri and ultrasound radiation force in elastography: Applications to diagnosis and therapy . Proc IEEE . 96 : 490 - 2008 ;
- 13 . McDannold N , Maier SE . Magnetic resonance acoustic radiation force imaging . Med Phys . 35 : 3748 - 2008 ;
- 14 . Radicke M , Engelbertz A , Habenstein B , Lewerenz M , Oehms O , Trautner P , Weber B , Wrede S , Maier K . New image contrast method in magnetic resonance imaging via ultrasound . Hyperfine Interactions . 181 : 21 - 2008 ; 10.1007/s10751-008-9628-6
- 15 . Kaye EA , Chen J , Pauly KB . Rapid mr-arfi method for focal spot localization during focused ultrasound therapy . Magn Reson Med . 65 : 738 - 2011 ;
- 16 . Hertzberg Y , Volovick A , Zur Y , Medan Y , Vitek S , Navon G . Ultrasound focusing using magnetic resonance acoustic radiation force imaging: application to ultrasound transcranial therapy . Med Phys . 37 : 2934 - 2010 ;
- 17 . Chapman A , ter Haar G . Thermal ablation of uterine fibroids using mr-guided focused ultrasound-a truly non-invasive treatment modality . European Radiology . 17 : 2505 - 2007 ;
- 18 . Crouzet S , Murat FJ , Pasticier G , Cassier P , Chapelon JY , Gelet A . High intensity focused ultrasound (hifu) for prostate cancer: Current clinical status, outcomes and future perspectives . International Journal of Hyperthermia . 26 : 796 - 2010 ;
- 19 . Hynynen K , McDannold N , Vykhodtseva N , Jolesz FA . Noninvasive mr imaging-guided focal opening of the blood-brain barrier in rabbits . Radiology . 220 : 640 - 2001 ;
- 20 . Furusawa H , Namba K , Nakahara H , Tanaka C , Yasuda Y , Hirabara E , Imahariyama M , Komaki K . The evolving non-surgical ablation of breast cancer: Mr guided focused ultrasound (mrgfus) . Breast Cancer . 14 : 55 - 2007 ;
- 21 . Martin E , Jeanmonod D , Morel A , Zadicario E , Werner B . High-intensity focused ultrasound for noninvasive functional neurosurgery . Ann Neurol . 66 : 858 - 2009 ;
- 22 . Aubry JF , Tanter M , Gerber J , Thomas JL , Fink M . Optimal focusing by spatio-temporal inverse filter. ii. experiments. application to focusing through absorbing and reverberating media . J Acoust Soc Am . 110 : 48 - 2001 ;
- 23 . Marquet F , Pernot M , Aubry J-F , Montaldo G , Marsac L , Tanter M , Fink M . Non-invasive transcranial ultrasound therapy based on a 3d ct scan: protocol validation and in vitro results . Phys Med Biol . 54 : 2597 - 2009 ;
- 24 . Gateau J , Marsac L , Pernot M , Aubry J-F , Tanter M , Fink M . Transcranial ultrasonic therapy based on time reversal of acoustically induced cavitation bubble signature . IEEE Trans Biomed Eng . 57 : 134 - 2010 ;
- 25 . Aubry JF , Marsac L , Pernot M , Robert B , Boch AL , Chauvet D , Salameh N , Souris L , Darasse L , Bittoun J , Martin Y , Cohen-Bacrie C , Souquet J , Fink M , Tanter M . High intensity focused ultrasound for transcranial therapy of brain lesions and disorders . IRBM . 31 : 87 - 2010 ;

FIG. 1

MR-ARFI sequence used for the adaptive focusing of HIFU beams. Two rectangular bipolar MSG were added to a standard multislice spin-echo sequence with EPI readout. Two sonications were synchronized to the MSG periods.
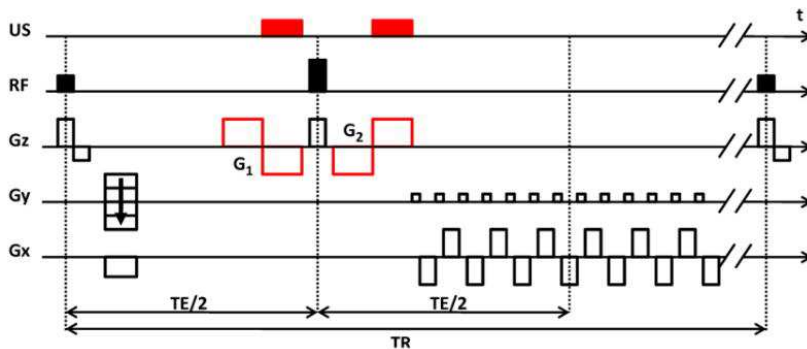

FIG. 2

(a) MR-ARFI phase image without US emission, (b) with US emission. (c) Final encoded displacement given by the difference of both images.
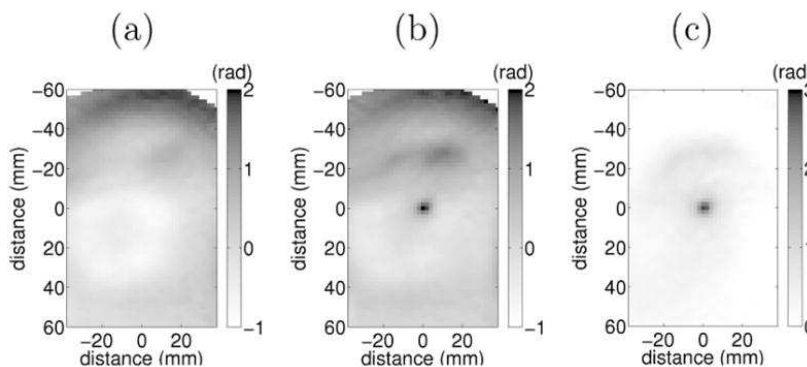
FIG. 3

(a) Representation of the 512 element HIFU transducer. The 384 elements used are plotted as round shapes and color intensity corresponds to the virtual skull phase aberration used. (b) Standard anatomic T1 weighted MR image of the setup (sagittal view) with schematic location of the probe in yellow, focus in red and MR-ARFI imaging plane in white. (c) Standard anatomic T1 weighted MR image of the calf brain sample in the MR-ARFI imaging plane with the MR-ARFI slice positioning in yellow, saturation bands in blue and probe focus in red.
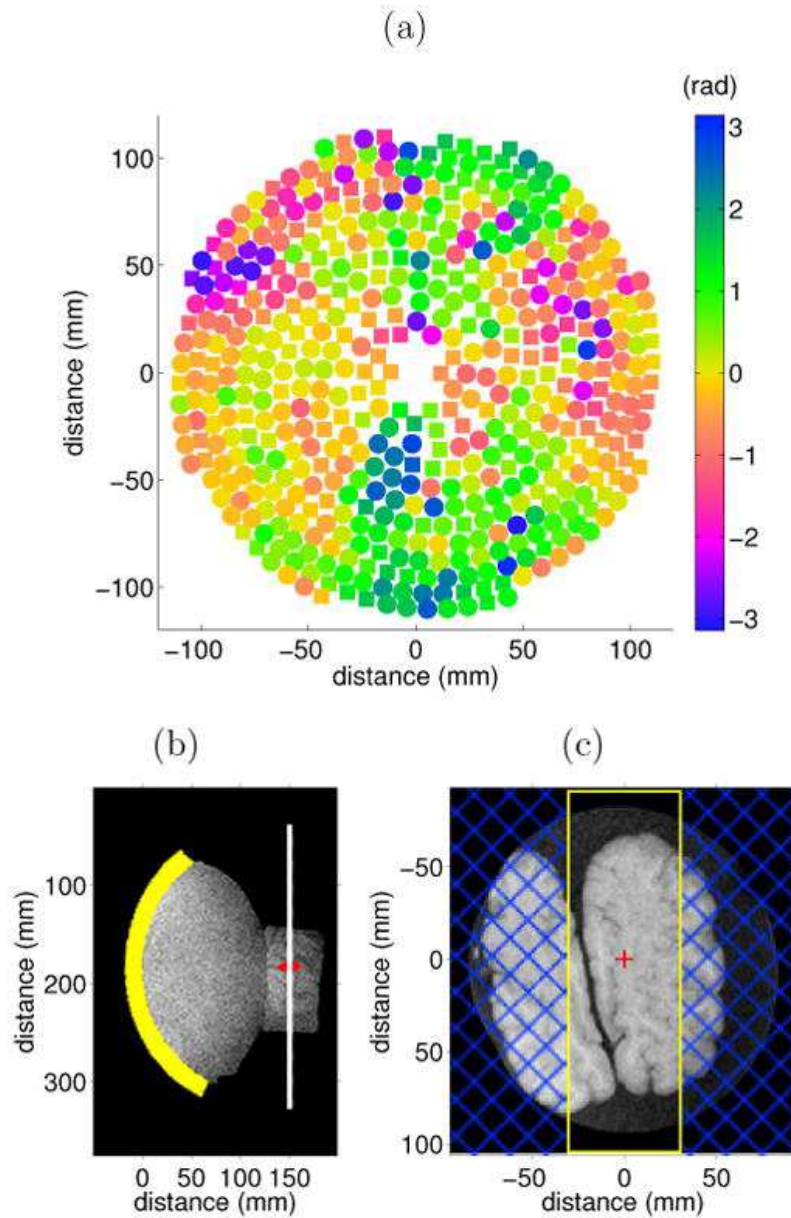
FIG. 4

T1 weighted image of the human cadaver head in the MR-ARFI imaging plane with MR-ARFI slice positioning in yellow, saturation bands in blue and probe focus in red.
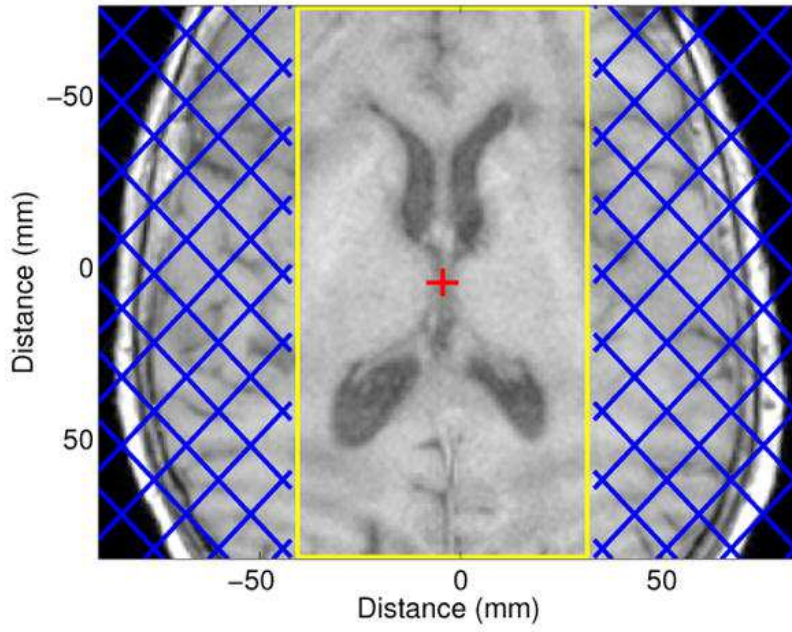
FIG. 5
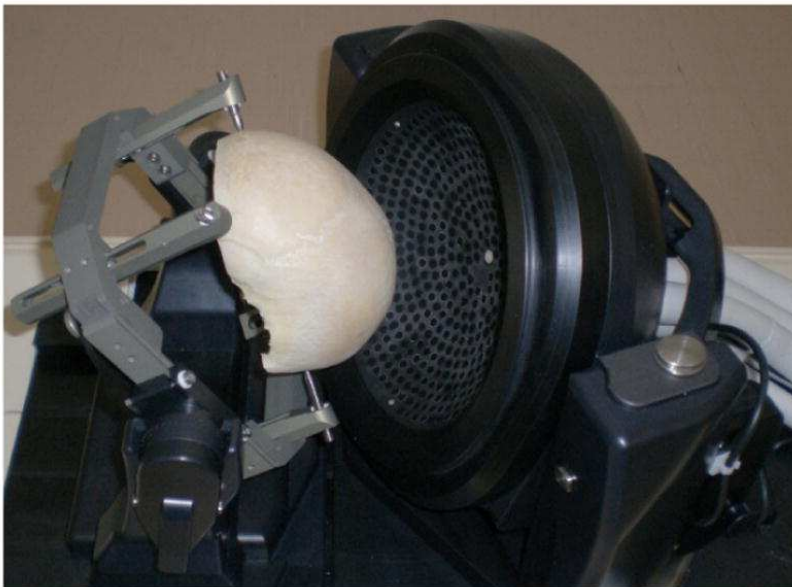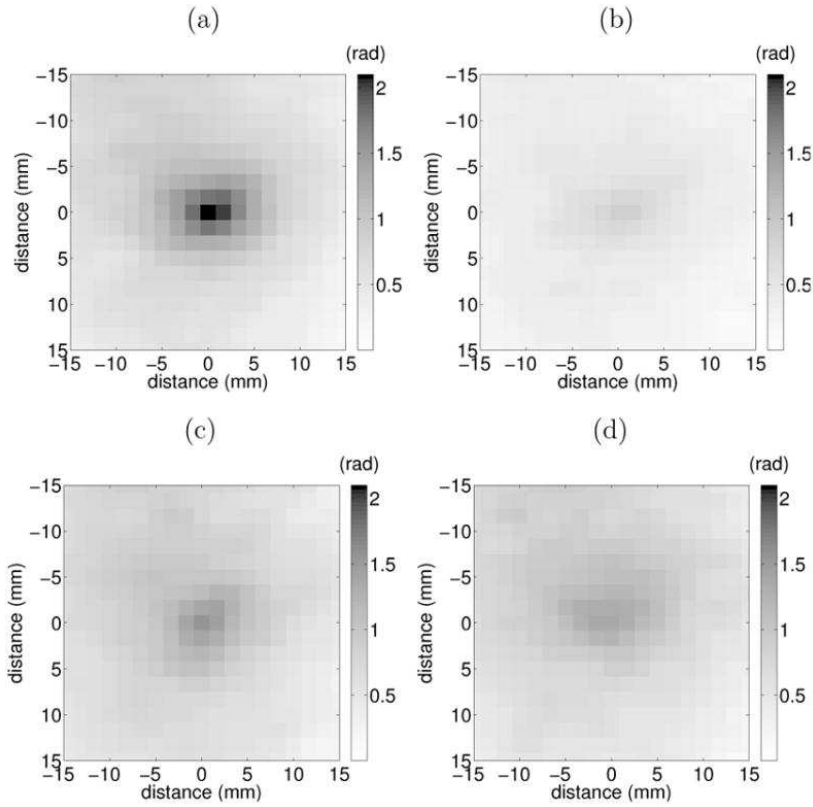
Illustration of the experimental setup.

FIG. 6

Example of encoded displacement (a), (b), (c) and (d) respectively for emission vectors 1, 6, 7 and 8.

FIG. 7

MR-ARFI encoded displacement obtained with: (a) aberration, (b) no aberration, (c) aberration and energy-based adaptive focusing correction. (d) Lateral profiles of the slices.
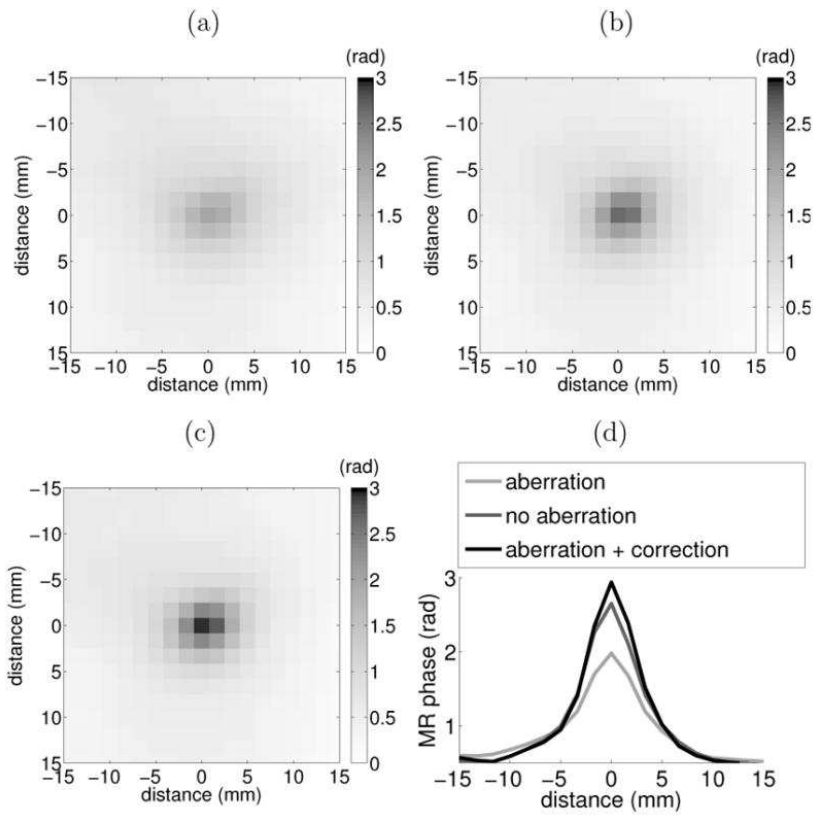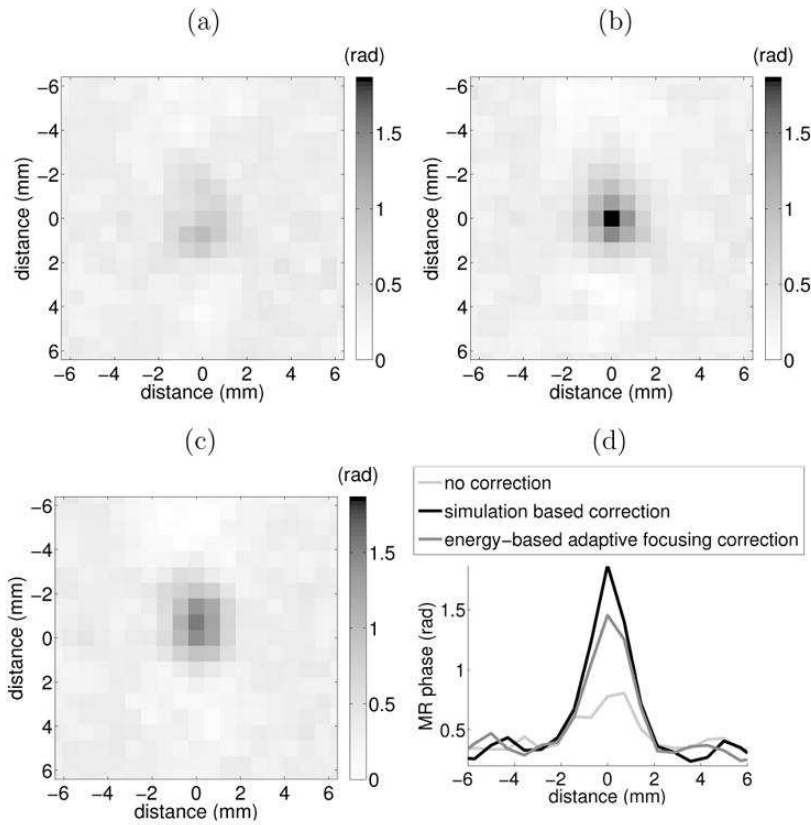
FIG. 8

MR-ARFI encoded displacement obtained with: (a) no correction, (b) simulation based correction, (c) energy-based adaptive focusing correction. (d) Lateral profiles of the slices.

FIG. 9

MR-ARFI encoded displacement obtained with: (a) no correction, (b) simulation based correction alone, (c) simulation based correction plus energy-based adaptive focusing correction. (d) Lateral profiles of the slices.
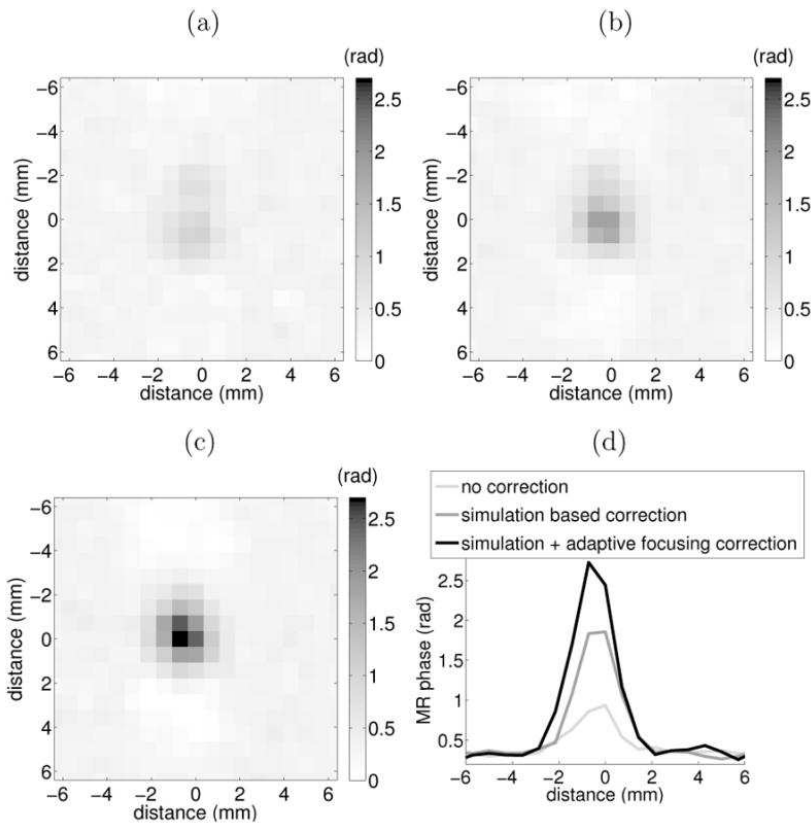
FIG. 10

Estimated acoustic intensity relative to the optimal focusing intensity.